

Article can be found under:

<http://dx.doi.org/10.1016/j.energy.2015.08.099>

Simulation and Evaluation of a Process Concept for the Generation of Synthetic Fuel from CO₂ and H₂

Daniel H. König, Nadine Baucks, Ralph-Uwe Dietrich, Antje Wörner

German Aerospace Center, Institute of Engineering Thermodynamics, Pfaffenwaldring 38-40, 70569 Stuttgart, Germany

Corresponding Author

German Aerospace Center
Institute of Engineering Thermodynamics
Daniel H. König
Pfaffenwaldring 38-40
70569 Stuttgart
Germany
Phone 0049 711 6862673
Email: daniel.koenig@dlr.de

KEYWORDS: Power-to-Liquid, Process Simulation, Synthetic Fuels, CO₂ utilization

HIGHLIGHTS:

- Process model of the generation of synthetic fuels from CO₂, power and H₂O developed.
- 100 MW_{LHV} of H₂ yields 1260 bbl/d of liquid hydrocarbon product.
- A Power-to-Liquid efficiency of 43.3% arises.
- Heat integration can reduce the energy losses to 25.6%.

ABSTRACT

Future aviation, shipping and heavy load transportation will continue to depend on energy carriers with a high energy density. The Power-to-Liquid technology is an approach to produce synthetic hydrocarbons, which fulfill this requirement. The proposed concept is based on H₂ from electrolysis, which reacts with CO₂ via the reverse water gas shift reaction to syngas. Syngas is then synthesized to liquid hydrocarbons by Fischer-Tropsch synthesis. A downstream product separation and upgrading section allows the production of defined fractions for specific applications. A flowsheet process model is build and heat integration is conducted. The input capacity is set to 100 MW_{LHV} of H₂. A total amount of 1260 *bbl/d* liquid hydrocarbons (67.1 MW_{LHV}) is generated. The carbon conversion and the Power-to-Liquid efficiency, which is defined as the fraction of the electrical energy chemically bound into liquid hydrocarbons, are identified as the parameters to evaluate the overall process performance. The Power-to-Liquid efficiency is found to be 43.3%. The carbon conversion rate of 73.7% indicates the exploiting of the introduced CO₂.

1. Introduction

The transportation and the energy sector depend globally mainly on fossil fuels. An increasing share of renewable energy production is observed in the energy sector. Nevertheless, the transportation sector is still fueled by nonrenewable resources. Crude oil covers today about 92% of the energy demand for transportation [1]. Moreover, the demand for transportation fuels is likely to increase by about 30 % or 10 EJ by 2050. This prediction foresees a doubling of the demand for diesel fuel and a triplication of the jet fuel demand by 2050 [2]. The rising consumption faces finite reserves of crude oil, which are forecasted to last for the next 34 to 40 years [3].

Today, compressed or liquefied natural gas is used as transportation fuel for motor vehicles as alternative to crude oil based liquid fuels. Natural gas can be synthesized by methanation from renewable hydrogen, called Power-to-Gas [4], [5]. However, aviation, shipping and heavy-load transportation depend on fuels with a high volumetric energy density [6]. The volumetric energy density of compressed natural gas is about a fifth of that of liquid fuels. For liquefied natural gas, the difference reduces to about one half of the volumetric energy density of liquid fuels. Research on alternative propulsion technologies for heavy-load transportation focuses on hybrid systems like the hydraulic hybrid vehicle technology, which still relies on liquid fuels [7]. In the maritime sector, fuel consumption is reduced by optimizing the cruising speed on shipping routes. Alternative fuel concepts comprise the use of liquefied natural gas from fossil resources [8]. Conventional aircrafts can be operated also on a long-term perspective only by liquid fuels. As a consequence, an increase of activities on blended biofuels and synthetic fuels is observed in the aviation industry in order to decrease the consumption of crude oil based fuels [9], [10]. Alternative fuels like hydrogen cannot be introduced without conceptual changes in aircraft and engine design as well as in infrastructure [11].

To secure the supply of liquid fuels for airborne, maritime and land applications, synthetic fuels from resources other than crude oil must be provided. The production of synthetic fuels is dominated by processes, which produce syngas followed by a synthesis process step to liquid hydrocarbons. One of the major technologies to convert syngas into synthetic liquid fuels is the Fischer-Tropsch (FT) synthesis. FT synthesis is an energy intense process with a wide variety of products requiring a complex product upgrading section [12]. However, liquid FT fuels can directly be used in the existing transportation infrastructure or as drop-in fuel to reduce the share of crude oil based fuels. Existing conventional routes utilize natural gas or coal as feedstock for the generation of syngas. These technologies are known as Gas-to-Liquid (GtL) and Coal-to-Liquid (CtL). The depletion time of natural gas and coal reserves exceeds the one of crude oil by approximately 1.75 and 5, respectively [3]. Nevertheless, those resources are also finite. Therefore, sustainable and renewable processes converting biomass to high quality fuels are currently under investigation. In principle, those process concepts include biomass gasification, a gas cleaning and conditioning section, the synthesis reaction step and a separation and upgrading section of the synthesis product to the desired biofuels (gasoline, kerosene and diesel). Techno-economic analyses of these Biomass-to-Liquid (BtL) processes were carried out in literature. The efficiency depends on the process concept, technologies and operation parameters and it varies between 33% – 50 % [13], [14], [15], [16], [17]. The potential and availability of biomass is limited [18]. The long-term idea of a closed-loop carbon cycle drew the attention to concepts that use H₂ and CO₂ as feedstock [19] [20] [21]. One option is the separation from industrial sources,

such as cement or iron and steel plants. By the application of carbon dioxide capture methods 932 Mt and 646 Mt of CO₂ could annually be separated from effluent gases of the cement industry and the iron and steel industry, respectively [22]. The production of synthetic fuels from solar energy and CO₂ was investigated by [23]. The study carried out a detailed techno-economic assessment of the production of methanol. Becker et al. [24] and Stempien et al. [25] conducted a thermodynamic analysis of the combination of the co-electrolysis of steam and CO₂ in a solid oxide electrolyzer cell with Fischer-Tropsch synthesis. The techno-economic performance of various gaseous and liquid fuels was analyzed by Tremel et al. [26], where the overall efficiencies of the respective processes were based on literature values. The study did not investigate the processes in detail and did not account for heat recovery and by-product use. Pilot or testing plants show early efforts to commercialize the Power-to-Liquid concept [27] [28]. For industrial application at larger scale, new developments and technical parameters, such as efficiencies, need to be revised and implemented. The objective of this work is to evaluate a process concept, which utilizes captured CO₂ and combines it with H₂ to produce liquid fuels. Based on the concept, the process components are selected and modeled with literature data. The model allows detailed insight into the interrelation of the single units and their effect on the overall process. The flowsheet model is developed in the flowsheet and process simulation software Aspen Plus®. A pinch point analysis is carried out with Aspen Energy Analyzer® to set up a heat integration network and determine the required utility loads.

2. Process Description

In general, Fischer-Tropsch based synthetic fuel production processes consist of three main process steps: syngas generation including gas conditioning, Fischer-Tropsch (FT) synthesis and product separation and upgrading. Additional process steps are waste water treatment, exhaust gas treatment and solid waste extraction [29]. **Fehler! Verweisquelle konnte nicht gefunden werden.** depicts a simplified block diagram of the process concept under investigation.

Fehler! Verweisquelle konnte nicht gefunden werden. illustrates the flowsheet of the process concept. The capacity of the plant is set to 100 MW of hydrogen input based on the lower heating value (LHV). This corresponds to the current and planned scale of large renewable energy installations, for instance wind farms or solar power stations. H₂ is produced by electrolysis, which is powered by these renewable energies. The mass flow of the H₂ feed (S-3) is calculated to equal the energy input of 100 MW. It was assumed that CO₂ (S-1) is provided at 0.1 MPa and 20°C. It is compressed by a multi-stage compressor to the required process pressure of 2.5 MPa. The reactants H₂ and CO₂ are mixed and preheated (S-4). The preheated feed is then mixed with the external recycle (S-18) and additional steam to increase the chemical conversion of the entire process and to adjust the reaction conditions for the downstream high temperature reformer (RWGS). The external recycle is a split of the total recycle stream (S-17). The recycle concept consisting of the external and internal recycle was applied to increase the overall carbon conversion. The combined stream (S-5) is fed to the RWGS. Water is knocked-out from the reformer product gas (S-6) before it is mixed with the internal recycle (S-19). The mixed stream (S-9) is heated to FT reaction temperature of 225 °C and fed to the FT reactor (FTS). A gaseous (S-10) and liquid (S-09) output stream are generated. The products of the FT synthesis are called syncrude [29] [12]. While the liquid product stream consists solely of syncrude the gas stream is

composed of the gaseous syncrude, unreacted reactants and inert components. The liquid stream is further supplied to the hydrocracker. The gaseous stream is cooled stepwise and simultaneously flashed (F-1 through F-4). Stepwise cooling at the pressure of the FT reactor is a widespread method of syncrude recovery and separation of gases and reaction water [15]. After the last separation stage (F-4 and C-2) the total recycle stream is split into the internal recycle, the external recycle and a fuel gas stream (FG-1). The fuel gas streams (FG-1 through FG-4) are the fuel supply of the burner of the RWGS. The liquid product (S-20) of the first flash (F-1) is split into a liquid phase (S-27) and waxy phase. The light waxes are combined with the liquid syncrude and supplied to the hydrocracker (S-21). The hydrocracker product (S-22) is flashed by F-7 to ambient conditions. The liquid products of the separation sections C-1, C-2, F-2 and F-3 are collected and brought to ambient conditions as well (F-6, F-5). S-24 represents a condensate at -15°C , S-25 a condensate at 40°C , S-26 a condensate at 70°C and S-27 a condensate at 150°C . These liquid streams are mixed to form the final liquid fuel.

3. Simulation Model

To assess and evaluate the generation of synthetic liquid fuels from CO_2 and H_2 a flowsheet simulation model has been developed in Aspen Plus®. Reaction rates are based on the thermodynamic equilibrium. A pressure drop of 0.3 MPa for the recycle stream is estimated [30] to account for pressure losses in the process. Heat losses of reactors, heat exchangers and piping are neglected.

3.1. Components and Thermodynamic Model

The model is based on pure components to describe the chemical reactions and the properties of mixtures within the process. H_2 , CO_2 , CO , H_2O and the n-alkanes CH_4 through $\text{C}_{30}\text{H}_{62}$ were selected from the Aspen database. Additionally the n-alkanes $\text{C}_{32}\text{H}_{66}$ and $\text{C}_{36}\text{H}_{74}$ were selected. Solid carbon represents coke to account for coke formation in the corresponding process steps. Air is composed out of 79% of N_2 and 21% of O_2 .

It is assumed that the gasoline, kerosene, diesel and wax fractions are represented by n-alkanes, since the main product of cobalt based low temperature FT synthesis are n-alkanes [12] [31]. **Fehler! Verweisquelle konnte nicht gefunden werden.** displays the hydrocarbon chain length definitions for the corresponding product fraction.

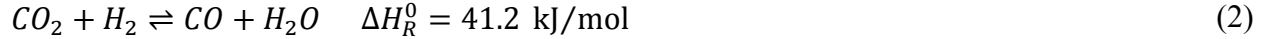
Thermodynamic property models are used to describe the chemical and physical behavior as well as the phase equilibrium of pure components and mixtures. In this work the Peng-Robinson equation of state in combination with the Boston-Mathias alpha function are used to describe the phase behavior in the process. The Peng-Robinson [32] equation of state is widely applied in the fields of gas processing, refining and synthetic hydrocarbon production [31] [33] [34] [35]. The alpha function derived by Boston and Mathias is applied at temperatures higher than the critical temperature and is useful for the description of light gases [36].

3.2. Syngas preparation - RWGS

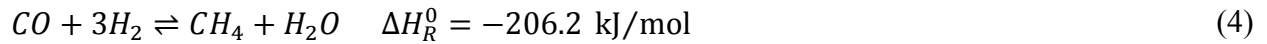
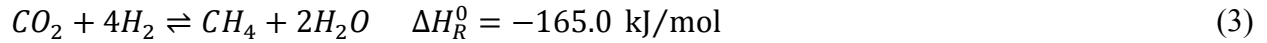
The reactant CO₂ is a highly stable molecule. It requires a substantial amount of energy, high temperatures and active catalysts for its chemical conversion [37]. The conversion of pure CO₂ to CO and O₂ (1) requires a large amount of energy.



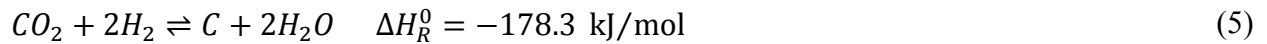
Combining CO₂ with a co-reactant such as H₂ the energy demand can be reduced. This reaction is the hydrogenation of CO₂ by the reverse water gas shift reaction (2), which is a heterogeneous catalyzed reaction:



Technically effective reaction conditions are realized in a reformer, which is equipped with fixed bed catalyst reactor tubes. Typical catalysts are based on nickel [38]. Due to the applied recycle concept to increase the conversion of the introduced carbon into hydrocarbons, the fresh feed of CO₂ and H₂ to the RWGS is mixed with a recycle stream consisting of light gases. These light gases are H₂, CO, CO₂, CH₄ and traces of longer hydrocarbons such as C₂H₆, C₃H₈ and C₄H₁₀. Furthermore steam is introduced to reduce coking in the reformer. Therefore, several parallel and side reactions apart from the reverse water gas shift reaction occur. These reactions are the Sabatier reaction (3) and the methanation reaction (4):



Unwanted side reactions which can lead to coking are the Bosch reaction (5) and Boudouard (6) reaction.



It was shown that at elevated temperatures the thermodynamic equilibrium is achieved for the reverse water gas shift reaction [38] [39] [40]. To account for all side reactions a reactor model, which is based on the minimization of the Gibbs energy, is chosen to model the RWGS reformer. The reactor temperature is fixed to 900 °C [38]. The pressure is set equal to the overall process pressure of 2.5 MPa to minimize compression work. Since reactions (4), (5) and (6) are thermodynamically not favored at high temperatures a steam mole fraction of $x_{H_2O} = 0.05$ is estimated to be sufficient to avoid coking in the RWGS [39]. Downstream the RWGS reactor a water knockout at 30 °C is included.

The burner provides the required temperature level and energy demand of the reaction. An adiabatic model, which is based on a Gibbs energy minimizing reactor model, is selected to model the burner. The fuel is provided by the internal generation of gaseous hydrocarbons and unreacted H₂. The heat of the hot flue gas is recovered. The exit temperature of the flue gas is set to 150 °C to avoid condensation.

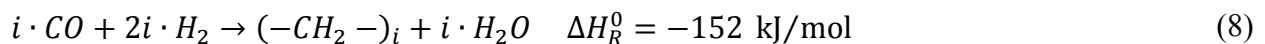
To increase the overall conversion a recycle is configured. The recycle is composed of unreacted reactants, inert components and light hydrocarbons and corresponds to S-17 in **Fehler! Verweisquelle konnte nicht gefunden werden.** As shown in **Fehler! Verweisquelle konnte nicht gefunden werden.** the recycle stream was split in three streams. The split fractions of the splitter (Split) are determined by the internal recycle (S-19) and the fuel gas stream (FG-1). The internal recycle is set by the FT operation parameters, see for details section 3.3. The fraction of the fuel gas stream is iteratively calculated by the required heat of the RWGS. The external recycle (S-18) is variable and calculated in dependence of FG-1 and S-19.

3.3. Fischer-Tropsch synthesis

The FT synthesis is a heterogeneous catalyzed reaction, which is categorized into high temperature and low temperature FT synthesis. High temperature FT synthesis is applied when the main products are alkenes or straight run fuels. Low temperature FT synthesis produces mainly hydrocarbons in the range of liquid waxes [29]. In this study low temperature FT synthesis was selected. In commercial plants, typically iron or cobalt based catalysts are employed. While the iron catalyst can either be used in the high or low temperature configuration, cobalt based catalysts are limited to low temperature FT processes [29]. The FT synthesis is defined as the process to convert syngas to synthetic crude oil. Syncrude can be composed of alkanes, alkenes, alcohols, carbonyls and carboxylic acids [12]. Beside these different compound classes also the corresponding homologous series of the compound classes are generated. The carbon number distribution describes the extent at which a particular compound is produced. The carbon number distribution is determined by the chain growth probability α . At constant reaction conditions the chain growth probability is a measure of the likelihood that either chain propagation or termination occurs at the catalyst surface. The relation of the chain growth probability and the carbon number distribution of the FT product is called the Anderson-Schulz-Flory (ASF) distribution. The ASF (7) relates the carbon number n and the chain growth probability α to the mass fraction of the particular compound with the same carbon number w_n . Increasing the chain growth probability of the FT synthesis will lead to longer chain hydrocarbons.

$$w_n = \frac{(1 - \alpha)}{\alpha} \cdot \alpha^n \cdot n \quad (7)$$

The chain growth probability and therefore the product distribution depend on the catalyst type and the reaction conditions. Typical chain growth probabilities for iron and cobalt catalysts are reported in the range of 0.50 – 0.70 and 0.70 – 0.95, respectively [41]. In this study a cobalt catalyst is selected. Application of the low temperature FT synthesis with a cobalt catalyst yield mainly alkanes as products [29]. Therefore, it was assumed that the generated syncrude is solely composed of linear alkanes. This assumption is reasonable in terms of significance of this work and was applied in several other studies as well [13] [31] [33] [42]. The synthesis of alkanes is formulated in (8).



The term $(-CH_2 -)_i$ represents a methylene group of the alkane chain with the length i . The FT reaction (8) is an exothermic reaction. To model the FT reactor a stoichiometric model is

selected and 32 reactions for the alkanes CH_4 through $\text{C}_{30}\text{H}_{66}$ and $\text{C}_{32}\text{H}_{74}$ and $\text{C}_{36}\text{H}_{74}$ are implemented. The respective fractional conversion of each reaction is calculated on basis of the ASF. The operating parameters of the FT reactor model are summarized in **Fehler! Verweisquelle konnte nicht gefunden werden.**

The overall CO conversion is increased by the described recycle configuration. The internal recycle (S-19) is led to the FT reactor to be mixed with the fresh feed from the RWGS. The split fraction of the internal recycle is calculated from the predefined fraction of reactants in the FT feed gas $f_{\text{H}_2+\text{CO}} \cdot R_{\text{H}_2/\text{CO}}$ is determined by adjusting the amount of fresh CO_2 feed to the process. There are two product streams of the FT reactor. One is composed of heavy hydrocarbons, which are liquid (S-9) at the reaction temperature and the other is composed of the gaseous products (S-10) and unreacted compounds.

3.3. Product separation and upgrading section

In the product upgrading section the syncrude is separated into five fractions, which are characterized by their boiling points and therefore by their chemical composition. The gaseous part of the syncrude and the included unreacted and reactive compounds are stepwise cooled and flashed, while the respective condensate is separated and forwarded as product fraction. In this work four separation steps (F-1 to F-4) are modeled. The temperature of the first flash (F-1) is set to $T_1 = 150^\circ\text{C}$, so that longer hydrocarbons are separated but no water condensation occurs in the flash drum. The longer hydrocarbons are expanded to ambient pressure and fractionated into two liquid streams in a distillation column (C-1). The light oil (S-27) includes hydrocarbons with a carbon number less than C_{20} . Hydrocarbons with a carbon number higher than C_{20} are collected as light waxes in the bottom of the column. In the second and third separation step (F-2 and F-3) the gases are cooled to $T_2 = 70^\circ\text{C}$ and $T_3 = 40^\circ\text{C}$, respectively [12]. In both flash drums water, which is produced during the FT synthesis, is separated as a second liquid phase from the hydrocarbons. The liquid streams (S-25 and S-26) are expanded to ambient pressure. The remaining gaseous stream of the third flash drum is cooled to $T_4 = -15^\circ\text{C}$ [12] and the liquid fraction is forwarded to a distillation column (C-2). Here hydrocarbons with a chain length C_5 and longer are separated from the gaseous compounds which include hydrocarbons with a chain length of C_4 and shorter. While the liquid stream is expanded to ambient pressure (S-24), the gaseous stream is mixed with the gases from the fourth flash drum and represents the recycle (S-17) of the process. The light waxes separated in F-1 were combined with the liquid syncrude (S-9). These waxes were compressed to the operation pressure of the hydrocracker, which is assumed to be 6.0 MPa and preheated to the operation temperature of $T_{\text{HC}} = 350^\circ\text{C}$ [45]. Hydrocracking is the catalytic cracking of longer hydrocarbons into desired fuel fractions. The cracking reaction is done in the presence of H_2 . The hydrocracker is modeled as a yield reactor with a given product distribution. The product distribution was taken from [46].

4. Results

4.1. Model results

The definitions and operation parameters described in the simulation model section are the basis for the calculations. The capacity was set to a fresh input flow of 100 MW of H₂ based on its LHV. The additional H₂ required by the hydrocracker is treated as an additional input. This corresponds to a total H₂ mass flow into the process of $\dot{m}_{\text{H}_2} = 3.01 \text{ t/h}$ (33,370 Nm³/h). **Fehler! Verweisquelle konnte nicht gefunden werden.** depicts a mass flow based block flow diagram of the process.

The specific energy consumption of a proton exchange membrane (PEM) electrolysis system is reported in the range of 4.5 – 7.5 kWh/Nm³. On a long-term perspective a specific system energy consumption of 4.1 – 4.8 kWh/Nm³ is expected [47]. In this work, a specific system energy consumption of 4.3 kWh/Nm³ is selected and it is assumed that the electrolysis is operated under the operational pressure of the plant. A DC electrical power input of 144.1 MW is needed resulting in a LHV based electrolysis efficiency of 69.7 %. The efficiency of the rectifier to convert alternate current into direct current, which is required by electrolysis, was assumed to 96 % [24]. The AC electrical power input into the electrolyzer is 150.1 MW. The total inlet flow of CO₂ is calculated to 22.9 t/h based on the RGWS and FT reaction conditions. A multi-stage compressor is modeled to compress the CO₂ at atmospheric pressure to the operation pressure 2.5 MPa. Three stage compression with intercooling is modeled and usual polytropic and mechanical efficiencies of 72% and 95% are assumed [48]. After mixing the fresh feed with the internal recycle and steam the CO₂ is hydrogenated with H₂ in the high temperature reformer. The heat demand of the endothermic reverse water gas shift reaction is determined to be 11.5 MW. This heat demand is provided by the burner. The burner is fueled by 3.9 t/h fuel gas, which is generated by the atmospheric flashes. Additionally 24.2 t/h of supply air are required and 28.1 t/h of flue gas are emitted.

The stepwise cooling and separation of the product of the FT reactor leads to five intermediate product streams. The fractional composition is shown in **Fehler! Verweisquelle konnte nicht gefunden werden.**. Depending on the separation temperature, the particular condensing hydrocarbons are collected and represent the respective fraction.

The fraction “Cracked” is the product of the hydrocracker and is composed of hydrocarbons in the chain length range between C₃ and C₁₅. The maximum is located at a chain length of C₉. The condensates at –15°C and 70°C represent with about 60% the largest share in the total product distribution. A total amount of 5.5 t/h (1260 bbl/d) of liquid fuels is generated in the process, which corresponds to a chemical energy of 67.1 MW_{LHV}. In accordance to **Fehler! Verweisquelle konnte nicht gefunden werden.** the final product can be fractionated into 3 transportation fuel types: gasoline, kerosene and diesel. Due to the assumption of taking only n-alkanes in consideration the fractions do not represent engine compatible fuels. But a good estimation is given, how the product of the proposed process concept would be divided into the corresponding fuel fractions. The results are shown in **Fehler! Verweisquelle konnte nicht gefunden werden.** Beside the hydrocarbon product the exothermic Fischer-Tropsch reaction generates heat (21.86 MW), which is converted into 40.6 t/h of steam at 225°C and 2.0 MPa. To account for the pressure drop within the process a single stage compressor was modeled. A polytropic efficiency of 72% and a mechanical efficiency of 95% were assumed. **Fehler! Verweisquelle konnte nicht gefunden werden.** summarizes the results of the flowsheet simulation.

4.2. Heat Integration

A pinch point analysis is performed to determine the utility requirements for cooling and heating of the process. The composite curve diagram shown in **Fehler! Verweisquelle konnte nicht gefunden werden.** illustrates the heating and cooling composite curves. As shown in **Fehler! Verweisquelle konnte nicht gefunden werden.** the heating demand of the cold streams can be satisfied by the hot streams of the process. Hence, no additional heat sources are needed. A target cooling demand of 44.9 MW is calculated. Refrigeration, cooling water, low pressure steam generation (LP steam) and medium pressure steam generation (MP steam) are identified to satisfy the required cooling demand of the process. Additionally, the heat generated by the exothermic FT reaction is used to generate steam (FT steam), which can be utilized within the process or in further processes. **Fehler! Verweisquelle konnte nicht gefunden werden.** lists the required types and corresponding cooling loads of the cooling applications.

Cooling water is taken from a river with a average annual temperature of 15°C and an allowed effluent temperature increase of 5°C. Assuming a pressure drop of 0.5 MPa for cooling water, 1.1 MW of electrical energy for pumping is required. Due to the different temperature levels of the hot streams in the process two different types of steam are generated beside the FT steam. The produced steam is excess heat, which could be used in other plants. As depicted by **Fehler! Verweisquelle konnte nicht gefunden werden.** and **Fehler! Verweisquelle konnte nicht gefunden werden.** 3.8 MW of the FT steam are used internally by the process. A vapor-compression refrigeration system is installed to cool down the stream S-13 to –15°C. Assuming an air cooled condenser at an air temperature of 45°C an ideal coefficient of performance (COP) of 3.5 was calculated. Taking the non-idealities into account a COP of 2.1 is determined [48] resulting in an electrical energy load for refrigeration of 0.5 MW.

4.3. Process Performance

Four parameters are defined to evaluate and compare the performance, chemical conversion and efficiency of the process. The overall efficiency relates the electrical energy input to the chemical energy content of the liquid products. It is defined as the Power-to-Liquid efficiency η_{PtL} (9).

$$\eta_{PtL} = \frac{\dot{m}_{SF} \cdot LHV_{SF}}{P_{EL} + P_U} \quad (9)$$

where \dot{m}_{SF} represents the mass flow of the generated synthetic fuels, which is multiplied by the related lower heating value LHV_{SF} . The electrical energy is represented by the part of electrical energy consumed by the electrolyzer (P_{EL}) and the part consumed by the utilities required in the process (P_U). The chemical conversion efficiency η_{CCE} (10) is specified as the efficiency of the chemical conversion of CO₂ and H₂ to liquid hydrocarbons.

$$\eta_{CCE} = \frac{\dot{m}_{SF} \cdot LHV_{SF}}{(\dot{m}_{H_2,FEED} + \dot{m}_{H_2,HC}) \cdot LHV_{H_2}} \quad (10)$$

The chemical energy of the products is calculated by $\dot{m}_{SF} \cdot LHV_{SF}$. The chemical energy of the introduced H₂ is the sum of the H₂ fed to the RWGS ($\dot{m}_{H_2,FEED}$) and the H₂ fed to the

hydrocracker ($\dot{m}_{H_2,HC}$) multiplied by LHV_{H_2} . Energy losses due to utilities are neglected. The chemical conversion of the carbon atom of CO_2 to synthetic fuels is defined as η_C

$$\eta_C = \frac{\dot{n}_{C,SF}}{\dot{n}_{C,FEED}} \quad (11)$$

where $\dot{n}_{C,SF}$ is the molar flow of carbon atoms in the synthetic hydrocarbons and $\dot{n}_{C,FEED}$ the molar flow of carbon atoms in the CO_2 feed stream. In PtL processes CO_2 is a valuable reactant, which must be purchased or separated by energy intense technologies from flue gases. Hence, the CO_2 conversion is a good measure to evaluate the efficiency of the conversion of CO_2 to liquid fuels. The mass based recycle ratio R is selected as the fourth evaluation parameter.

$$R = \frac{\dot{m}_{FEED} + \dot{m}_{RECYCLE}}{\dot{m}_{FEED}} \quad (12)$$

\dot{m}_{FEED} is the total mass flow of fresh feed and $\dot{m}_{RECYCLE}$ is the total mass flow of the respective recycle stream. The recycle ratio is introduced to rate the extend of recycling. **Fehler! Verweisquelle konnte nicht gefunden werden.** depicts the formulas of the recycle ratios under investigation. **Fehler! Verweisquelle konnte nicht gefunden werden.** summarizes the results of the flowsheet simulation and of the energy balance. Additionally, the results of the evaluation parameters are shown. R_{FTS} relates the internal recycle stream and the product stream of the RWGS, which represents the fresh feed to the FT synthesis. The ratio $R_{FTS} = 5.44$ indicates that the internal recycle stream is 4.44 times larger than the fresh feed from the RWGS. Analogous, R_{RWGS} was defined as the ratio of fresh feed to the RWGS plus the external recycle stream divided by the fresh feed. The fresh feed to the RWGS is about 2.56 times larger than the internal recycle. It results from $R_{TOTAL} = 6.03$ that the total recycle is 5.03 times larger than the fresh feed to the process. Recycle ratios in the range of $R_{TOTAL} = 2.56 - 4.48$ are reported for a per-pass CO conversion of 80% in the FT [49]. Applying a CO conversion of 80%, a R_{TOTAL} of 3.24 is determined in this work, which is in good agreement with the reported literature value. A chemical conversion efficiency of 66.8% is calculated for the process. The supply of the heat demand of the RWGS accounts for about 35% of the losses. 65% of the losses are excess heat of the FT reaction, which is converted into steam. Using the excess heat by processes with a significant heat demand, for instance carbon dioxide separation from flue gases could increase the overall efficiency dramatically. The chemical conversion efficiency of the process represents also the maximum efficiency of the conversion of H_2 and CO_2 to liquid fuels of the proposed concept. The Power-to-Liquid efficiency accounts for the losses by the electrolysis of water and utility loads. The energy losses of the electrolysis are 21.4%, the loss of the utilities are 2.1%. Thus, 43.3% of the introduced electrical energy can be converted into chemical energy in form of liquid hydrocarbon. 1260 bbl/d of liquid hydrocarbons could be produced with the assumed input capacity of 3.01 t/h H_2 .

4. Discussion

Recent research adapted the principle of natural photosynthesis to convert CO_2 and H_2O to hydrocarbon compounds using solar energy [50], [51]. Herron et al proposed the synthesis of methanol by photo-catalytic CO_2 reduction [23]. Conventional technologies are combined with

renewable energy sources to produce sustainable fuels [19], [52], [53], e.g. the combination of FT synthesis with steam co-electrolysis was investigated by Becker et al [24] and Stempien et al [25]. In contrast, this study combines a PEM electrolyzer with RWGS to decouple the H₂ production and the chemical plant.

Greenhouse gas emission free power sources are nuclear power and renewable power sources. Nuclear power generation is characterized by low electricity prices and high full load hours [54]. However, safety concerns and open questions of nuclear waste handling are still not entirely answered [55]. Therefore, this study focuses on renewable power technologies. The highest growth rates and future investments into the renewable power sector are expected for wind power and photovoltaics [56]. They depend on natural conditions, namely the wind speed and the solar irradiation and on the day-night rhythm. These renewable technologies are characterized by a fluctuating generation pattern following natural conditions. Therefore, the fluctuating power source must be coupled with the stationary synthesis process by an intermediate storage to balance the dynamic power generation.

The proposed PEM electrolyzer is characterized by the ability to cover large power density ranges and is able to follow the power generation pattern of renewable energy resources [57]. In combination with hydrogen storage in caverns PEM electrolysis is a technology option to link the fluctuating power and the stationary synthesis. The option of a hydrogen grid, where hydrogen is supplied to chemical plants, was discussed elsewhere [26]. The annual capacity factors have to be considered for using renewable electricity generation. Photovoltaic has a typical capacity factor between 20 % and 30 %. The capacity factors for wind power range from 20 % – 50 % [58]. If the proposed plant shall be powered solely by wind power, a minimum of twice the installed electrolyzer capacity will be required to produce the equal amount of fuel compared to a stationary power supply. The 100 MW_{LHV} H₂ plant requires annually about 1,315 GWh of electrical energy input. Current electricity costs for offshore wind power are reported to 160 US\$/MWh [59]. Taking only these electricity costs into account a synthetic fuel price of about 460 US\$/bbl arises, which is more than four times the average Brent crude oil spot price of 109 US\$/bbl in 2013 [60].

5. Conclusion

A concept to generate liquid hydrocarbon fuels from H₂ and CO₂ was presented. The process was modeled in Aspen Plus. The process model includes a reverse water gas shift reactor, a Fischer-Tropsch reactor, a hydrocracker and a product separation section. The energy and mass balances were calculated and a pinch point analysis was conducted. The carbon conversion and the Power-to-Liquid efficiency were identified as the parameters to evaluate the overall process. A Power-to-Liquid efficiency of 43.3% arises. The carbon conversion is calculated to be 73.7%. Additionally to the desired product, a total of 25.7 MW excess heat in form of steam (see **Fehler! Verweisquelle konnte nicht gefunden werden.**) is produced.

The production of synthetic liquid fuels from renewable power faces two major challenges. First, the fluctuation in the renewable power generation implicates low full load hours which require intermediate storage, fast response time of the electrolyzer and high installed capacities. Second,

the economics indicate high electricity price impact on the production cost. At electricity prices of about 38 *US\$/MWh* market price level may be obtained if capital costs are neglected. Further improvements regarding electrolyzer cost and efficiency, as well as general advances of plant construction are necessary to reach market entry level.

Based on a reasonable set of assumptions a specific solution and parameter set for the process concept has been generated. Sensitivity analyses will be part of a subsequent study to evaluate and optimize the Power-to-Liquid process concept. The chain growth probability (see equation (7)) will affect the share of intermediate product forwarded to the hydrocracker and subsequently the calculated production cost per barrel product. Therefore, an optimal match of technical feasible chain growth probability and hydrocracker product distribution will be investigated to meet current and future fuel demands. Additionally, the pressure of the RWGS will be optimized instead of linking it to the FT synthesis pressure. Its effect on the overall system efficiency will be investigated and the Power-to-Liquid efficiency optimized. Using the by-product steam internally to increase the overall efficiency is another option to be investigated, too. When an optimized process has been obtained, the production cost of liquid fuels from renewable sources can be assessed by a capital and operation cost estimation.

ACKNOWLEDGMENT

Financial support from the Helmholtz Association is gratefully acknowledged. This work is part of the Helmholtz Energy Alliance “Synthetic Liquid Hydrocarbons”.

NOMENCLATURE

AC	Alternate current
ASF	Anderson-Schulz-Flory distribution
α	Chain growth probability
BtL	Biomass-to-Liquid
COP	Coefficient of performance
CtL	Coal-to-Liquid
DC	Direct current
EL	Electrolysis
η_C	Carbon conversion
η_{CCE}	Chemical conversion efficiency
η_{PtL}	Power-to-Liquid efficiency
f_{H_2+CO}	Molar fraction of H ₂ and CO
FT	Fischer-Tropsch
FTS	Fischer-Tropsch synthesis reactor
GtL	Gas-to-Liquid
ΔH_R^0	Standard enthalpy of reaction (<i>kJ/mol</i>)
LHV	Lower Heating Value
LP	Low pressure steam
\dot{m}	Mass flow (<i>t/h</i>)
MP	Medium pressure steam
n	Carbon number
p	Pressure (<i>MPa</i>)
P	Power (<i>MW</i>)
PEM	Proton exchange membrane
PtL	Power-to-Liquid
R	Recycle ratio
$R_{H_2/CO}$	H ₂ -to-CO ratio
RWGS	High temperature reformer
SF	Synthetic fuel
T	Temperature (<i>°C</i>)
U	Utilities
w	Mass fraction

REFERENCES

- [1] International Energy Agency, "Key World Energy Statistics," International Energy Agency, Paris, 2014.
- [2] World Energy Council, "Global Transport Scenarios 2050," World Energy Council, London, 2011. ISBN:978-0-946121-14-4.
- [3] S. Shafiee and E. Topal, "When Will Fossil Fuel Reserves be Diminished?," *Energy Policy*, no. 37, pp. 181-189, 2009. DOI:10.1016/j.enpol.2008.08.016.
- [4] J. Stempien, M. Ni, Q. Sun and S. Chan, "Production of sustainable methane from renewable energy and captured carbon dioxide with the use of solid oxide electrolyzer: A thermodynamic assessment," *Energy*, vol. 82, pp. 714-721, 2015. DOI:10.1016/j.energy.2015.01.081.
- [5] E. Giglio, A. Lanzini, M. Santarelli and P. Leone, "Synthetic natural gas via integrated high temperature electrolysis and methanation: Part I - Energy performance," *J. of Energy Storage*, vol. 1, pp. 22-37, 2015. DOI:10.1016/j.est.2015.04.002.
- [6] R. Pietzcker, T. Longden, W. Chen, S. Fu, E. Kriegler, P. Kyle and G. Luderer, "Long-term transport energy demand and climate policy: Alternative visions on transport decarbonization in energy-economy models," *Energy*, vol. 64, pp. 95-108, 2014. DOI:10.1016/j.energy.2013.08.059.
- [7] Z. Filipi, L. Louca, B. Daran, C.-C. Lin, U. Yildir, B. Wu, M. Kokkolaras, D. Assanis, H. Peng, P. Papalambros, J. Stein, D. Szkubiel and R. Chapp, "Combined Optimisation of Design and Power Management of the Hydraulic Hybrid Propulsion System for the 6 × 6 Medium Truck," *Int. J. Heavy Vehicle Systems*, no. 11, 2004. DOI:10.1504/IJHVS.2004.005458.
- [8] K. Fagerholt, G. Laporte and I. Norstad, "Reducing Fuel Emissions by Optimizing Speed on Shipping Routes," *J. Operational Research Society*, no. 61, pp. 523-529, 2010. DOI:10.1057/jors.2009.77.
- [9] J. Hileman and R. Stratton, "Alternative jet fuel feasibility," *Transport Policy*, no. 34, pp. 52-62, 2014. DOI:10.1016/j.tranpol.2014.02.018.
- [10] P. Trivedi, H. Olcay, M. Staples, M. Withers, R. Malina and S. Barrett, "Energy return on investment for alternative jet fuels," *Applied Energy*, vol. 141, pp. 167-174, 2015. DOI:10.1016/j.apenergy.2014.12.016.
- [11] D. Daggett, O. Hadaller, R. Hendricks and R. Walther, "Alternative Fuels and their Potential Impact on Aviation," National Aeronautics and Space Administration, Cleveland, OH, 2006.

- [12] A. de Klerk, Fischer-Tropsch Refining, Weinheim: Wiley-VCh Verlag, 2011. ISBN:978-3-527-32605-1.
- [13] C. Hamelinck, A. Faaij, H. den Uil and H. Boerrigter, "Production of FT Transportation Fuels from Biomass; Technical Options, Process Analysis and Optimisation, and Development Potential," *Energy*, no. 29, pp. 1743-1771, 2004. DOI:10.1016/j.energy.2004.01.002.
- [14] R. Swanson, A. Platon, J. Sapiro and R. Brown, "Techno-economic Analysis of Biomass-to-Liquids Production Based on Gasification," *Fuel*, vol. 89, pp. 11-19, 2010. DOI:10.1016/j.fuel.2010.07.027.
- [15] M. Tijmensen, A. Faaij, C. Hamelinck and M. van Hardeveld, "Exploration of the Possibilities for Production of Fischer Tropsch Liquids and Power via Biomass Gasification," *Biomass Bioenergy*, no. 23, pp. 129-152, 2002. DOI:10.1016/S0961-9534(02)00037-5.
- [16] F. Trippe, M. Fröhling, F. Schultmann, R. Stahl, E. Henrich and A. Dalai, "Comprehensive techno-economic assessment of dimethyl ether (DME) synthesis and Fischer-Tropsch synthesis as alternative process steps within biomass-to-liquid production," *Fuel Processing Technology*, vol. 106, pp. 577-586, 2013. DOI:10.1016/j.fuproc.2012.09.029.
- [17] D. Connolly, B. Mathiesen and I. Ridjan, "A comparison between renewable transport fuels that can supplement or replace biofuels in a 100% renewable energy system," *Energy*, vol. 73, pp. 110-125, 2015. DOI:10.1016/j.energy.2014.05.104.
- [18] D. van Vuuren, J. van Vliet and E. Stehfest, "Future Bio-energy Potential under Various Natural Constraints," *Energy Policy*, vol. 37, pp. 4220-4230, 2009. DOI:10.1016/j.enpol.2009.05.029.
- [19] C. Graves, S. Ebbesen, M. Mogensen and K. Lackner, "Sustainable Hydrocarbon Fuels by Recycling CO₂ and H₂O with Renewable or Nuclear Energy," *Renewable and Sustainable Energy Reviews*, vol. 15, pp. 1-23, 2011. DOI:10.1016/j.rser.2010.07.014.
- [20] D. Mignard and C. Pritchard, "Processes for the Synthesis of Liquid Fuels from CO₂ and Marine Energy," *Chemical Engineering Research and Design*, vol. 84, pp. 828-836, 2006. DOI:10.1205/cherd.05204.
- [21] I. Ridjan, B. Mathiesen and D. Connolly, "Synthetic fuel production costs by means of solid oxide electrolysis cells," *Energy*, vol. 76, pp. 104-113, 2014. DOI:10.1016/j.energy.2014.04.002.
- [22] B. Metz, O. Davidson, H. de Coninck, M. Loos and L. Meyer, Eds., Carbon Dioxide Capture and Storage, New York: Cambridge University Press, 2005. ISBN:978-0-521-86643-9.

- [23] J. Herron, J. Kim, A. Upadhye, G. Huber and C. Maravelias, "A general framework for the assessment of solar fuel technologies," *Energy Environ. Sci.*, vol. 8, pp. 126-157, 2015. DOI:10.1039/c4ee01958j.
- [24] W. Becker, R. Braun, M. Penev and M. Melaina, "Production of Fischer-Tropsch Liquid Fuels from High Temperature Solid Oxide Co-Electrolysis Units," *Energy*, pp. 99-115, 2012. DOI:10.106/j.energy.2012.08.047.
- [25] J. Stempien, M. Ni, Q. Sun and S. Chan, "Thermodynamic analysis of combined solid oxide electrolyzer and Fischer-Tropsch processes," *Energy*, vol. 81, pp. 682-690, 2015. DOI:10.1016/j.energy.2015.01.013.
- [26] A. Tremel, P. Wasserscheid, M. Baldauf and T. Hammer, "Techno-economic analysis for the synthesis of liquid and gaseous fuels based on hydrogen production via electrolysis," *Int. J. Hydrogen Energy*, p. in press, 2015. DOI:10.1016/j.ijhydene.2015.01.097.
- [27] Air Fuel Synthesis Ltd., "Air Fuel Synthesis," 2014. [Online]. Available: <http://www.airfuelsynthesis.com/>. [Accessed 18 05 2015].
- [28] W. Verdegaal, S. Becker and C. von Olshausen, "Power-to-Liquid: Synthetisches Rohöl aus CO₂, Wasser und Sonne," *Chemie Ingenieur Technik*, vol. 87, pp. 340-346, 2015. DOI:10.1002/cite.201400098.
- [29] A. Steynberg and M. Dry, Eds., Fischer-Tropsch Technology, Amsterdam: Elsevier B.V., 2004. ISBN:978-0-444-51354-0.
- [30] S. Hall, Rules of thumb for chemical engineers, 5 ed., Waltham: Butterworth-Heinemann, 2012. ISBN:978-0-12-387785-7.
- [31] M. Sudiro and A. Bertucco, "Production of Synthetic Gasoline and Diesel Fuel by Alternative Processes Using Natural Gas and Coal: Process Simulation and Optimization," *Energy*, no. 34, pp. 2206-2214, 2009. DOI:10.1016/j.energy.2008.12.009.
- [32] D. Peng and D. Robinson, "A New Two-constant Equation of State," *Ind. Eng. Chem. Fundam.*, no. 15, pp. 59-64, 1976. DOI:10.1021/i160057a011.
- [33] M. Sudiro and A. Bertucco, "Synthetic Fuels by a Limited CO₂ Emission Process which Uses Both Fossil and Solar Energy," *Energy & Fuels*, vol. 21, pp. 3668-3675, 2007. DOI:10.1021/ef7003255.
- [34] R. Baliban, J. Elia and C. Floudas, "Toward Novel Hybrid Biomass, Coal, and Natural Gas Processes for Satisfying Current Transportation Fuel Demands 1: Process Alternatives, Gasification Modeling, Process Simulation and Economic Analysis," *Ind. Eng. Chem. Res.*, no. 49, pp. 7343-7370, 2010. DOI: 10.1021/ie100063y.
- [35] J. Elia, R. Baliban and C. Floudas, "Toward Novel Hybrid Biomass, Coal, and Natural Gas Processes for Satisfying Current Transportation Fuel Demands 2: Simultaneous Heat and

- Power Integration," *Ind. Eng. Chem. Res.*, no. 49, pp. 7371-7388, 2010. DOI:10.1021/ie100064q.
- [36] J. Boston and P. Mathias, "Phase Equilibria in a Third-Generation Process Simulator," *Proceedings of the 2nd International Conference on Phase Equilibria and Fluid Properties in the Chemical Process Industries*, pp. 823-849, 17-21 March 1980.
- [37] C. Song, A. Gaffney and K. Fujimoto, Eds., *CO₂ Conversion and Utilization*, vol. 809, Washington D.C.: American Chemical Society, 2002. DOI:10.021/bk-2002-0809.
- [38] R. Unde, "Kinetics and Reaction Engineering Aspects of Syngas Production by the Heterogeneously Catalysed Reverse Water Gas Shift Reaction," 2012.
- [39] A. Jess, P. Kaiser, C. Kern, R. Unde and C. von Olshausen, "Considerations Concerning the Energy Demand and Energy Mix of Global Welfare and Stable Ecosystems," *Chemie Ingenieur Technik*, vol. 83, pp. 1777-1791, 2011. DOI:10.1002/cite.201100066.
- [40] W. Kim, D. Yang, D. Moon and B. Ahn, "The Process Design and Simulation for the Methanol Production on the FPSO (Floating Production, Storage and Off-loading) System," *Chemical Engineering Research and Design*, vol. 92, pp. 931-940, 2014. DOI:10.1016/j.cherd.2013.08.009.
- [41] G. van der Laan, "Kinetics, Selectivity and Scale Up of the Fischer-Tropsch Synthesis," Groningen, 1999.
- [42] K. Müller, J. Geng and W. Arlt, "Reversible vs. Irreversible Conversion of Hydrogen: How to Store Energy Efficiently?," *Energy Technology*, no. 1, pp. 42-47, 2013. DOI:10.1002/ente.201200022.
- [43] D. König, N. Baucks, G. Kraaij and A. Wörner, "Entwicklung und Bewertung eines Verfahrenskonzeptes zur Herstellung flüssiger Kohlenwasserstoffe unter Nutzung von CO₂," *Chemie Ingenieur Technik*, no. 86, p. 1351, 2014. DOI:10.1002/cite.201450066.
- [44] P. Kaiser, F. Pöhlmann and A. Jess, "Intrinsic and Effective Kinetics of Cobalt-Catalyzed Fischer-Tropsch Synthesis in View of a Power-to-Liquid Process Based on Renewable Energy," *Chemical Engineering Technology*, vol. 37, pp. 964-972, 2014. DOI:10.1002/ceat.201300815.
- [45] Y. Liu, K. Murata, K. Okabe, M. Inaba, I. Takahara, T. Hanaoka and K. Sakanishi, "Selective hydrocracking of Fischer-Tropsch waxes of high-quality Diesel fuel over Pt-promoted polyoxocation-pillared montmorillonites," *Top Catal*, vol. 52, pp. 597-608, 2009. DOI:10.1007/s11244-009-9239-8.
- [46] H. Coonradt and W. Garwood, "Mechanism of Hydrocracking," *I&EC Process Design and Development*, vol. 3, pp. 38-45, 1964. DOI:10.1021/i260009a010.

- [47] T. Smolinka, M. Günther and J. Garche, "Stand und Entwicklungspotenzial der Wasserelektrolyse zur Herstellung von Wasserstoff aus regenerativen Energien," NOW GmbH, Berlin, 2010.
- [48] R. Smith, *Chemical Process Design and Integration*, West Sussex: John Wiley & Sonms Ltd, 2005. ISBN:978-0-471-48681-7.
- [49] T. Kreutz, E. Larson, G. Liu and R. Williams, "Fischer-Tropsch Fuels from Coal and Biomass," Princeton University, Princeton, 2008.
- [50] Y. Izumi, "Recent advances in the photocatalytic conversion of carbon dioxide to fuels with water and/or hydrogen using solar energy and beyond," *Coordination Chemistry Reviews*, vol. 257, pp. 171-186, 2013. DOI:10.1016/j.ccr.2012.04.018.
- [51] I. Ganesh, "Solar fuels vis-a-vis electricity generation from sunlight: The current state-of-the-art (a review)," *Renewable and Sustainable Energy Reviews*, vol. 44, pp. 904-932, 2015. DOI:10.1016/j.rser.2015.01.019.
- [52] I. Ridjan, B. Mathiesen, D. Connolly and N. Duic, "The feasibility of synthetic fuels in renewable energy systems," *Energy*, vol. 57, pp. 76-84, 2013. DOI:10.1016/j.energy.2013.01.046.
- [53] G. Haarlemmer, G. Boissonnet, E. Peduzzi and P.-A. Setier, "Investment and production costs of synthetic fuels - A literature survey," *Energy*, vol. 66, pp. 667-676, 2014.
- [54] R. El-Emam, H. Ozcan and I. Dincer, "Comparative cost evaluation of nuclear hydrogen production methods with the Hydrogen Economy Evaluation Program," *Int. J. of Hydrogen Energy*, p. in press, 2015. DOI:10.1016/j.ijhydene.2014.12.098.
- [55] C. Poinssot, S. Bourg, N. Ouvrier, N. Combernoux, C. Rostaing, M. Vargas-Gonzalez and J. Bruno, "Assessment of the environmental footprint of nuclear energy systems. Comparison between closed and open fuel cycles," *Energy*, vol. 69, pp. 199-211, 2014. DOI:10.1016/j.energy.2014.02.069.
- [56] International Energy Agency, "World Energy Investment Outlook," International Energy Agency, Paris, 2014.
- [57] M. Carmo, D. Fritz, J. Mergel and D. Stolten, "A comprehensive review on PEM water electrolysis," *Int. J. Hydrogen Energy*, vol. 38, pp. 4901-4934, 2013. DOI:10.1016/j.ijhydene.2013.01.151.
- [58] Intergovernmental Panel on Climate Change, "Renewable Energy Sources and Climate Change Mitigation," Cambridge University Press, New York, 2012. ISBN:978-1-107-02340-6.
- [59] G. Timilsina, G. van Kooten and P. Narbel, "Global wind power development: Economics

and policies," *Energy Policy*, vol. 61, pp. 642-652, 2013. DOI:10.1016/j.enpol.2013.06.062.

[60] U.S. Energy Information Administration, "www.eia.gov," 2015. [Online]. Available: <http://www.eia.gov/dnav/pet/hist/LeafHandler.ashx?n=pet&s=rbrte&f=a>. [Accessed 28 05 2015].